DOI: 10.26599/FSHW.2025.9250896

Contents lists available at SciOpen

Food Science and Human Wellness

journal homepage: https://www.sciopen.com/journal/2097-0765

China Food Publishing Co.

In vitro fermentation characteristics of guar gum: Particularly enriching *Bifidobacterium pseudolongum* and *Parabacteroides distasonis*

Shanshan Zhang, Yonggan Sun, Yanli Zhang, Shaoping Nie *

State Key Laboratory of Food Science and Resources, China-Canada Joint Lab of Food Science and Technology, Key Laboratory of Bioactive Polysaccharides of Jiangxi Province, Nanchang University, Nanchang, 330047, China

ABSTRACT: Guar gum, a widely used food hydrocolloid, exhibits extensive biological activities and its regulatory effects on the gut microbiota are closely linked to health outcomes. However, its specific enrichment effects on gut microbiota and the interaction modes with the enriched bacteria remain unclear. This study investigated the regulatory effects using an *in vitro* fermentation model and both single-step and stepwise cultivation methods. Results showed that the gut microbiota degraded guar gum, yielding abundant acetate and propionate. Guar gum suppressed the growth of the potential pathogenic bacteria (Enterobacteriaceae) while enriching the beneficial bacteria (*Bifidobacterium* and *Parabacteroides*). Notably, *B. pseudolongum* and *P. distasonis* were specifically enriched, although neither could directly utilize guar gum. The primary degrader, such as *Bacteroides ovatus*, facilitated guar gum breakdown and stimulated the proliferation of *B. pseudolongum* and *P. distasonis*. Further analysis revealed that the proliferation of these bacteria may be related to their preferences for utilizing mannose and galactose. Taken together, these findings enhance our understanding of the interactions between guar gum and the microbiota, and contribute to the scientific basis for developing guar gum-based functional foods.

Keywords: guar gum, bioactive polysaccharides, gut microbiota, enrichment effect, *in vitro* fermentation, stepwise culture, SCFAs

1. Introduction

The gastrointestinal tract is colonized by a vast and complex microbial community that plays crucial physiological roles in regulating metabolism, promoting host immune system development, and preventing pathogen infection [1]. Increasing evidence suggests that gut microbiota dysbiosis can trigger chronic intestinal inflammation and contribute to the development of metabolic disorders and inflammatory bowel diseases (IBD) [2, 3]. Dietary factors are the key modulators of gut microbial structure [4]. With the shift in modern lifestyles, the consumption of highly processed foods has increased, and some food additives such as emulsifiers are often poorly absorbed and thus will likely directly interact with the microbiota [5]. Therefore, investigating the impact of emulsifiers on the gut microbiome is of great importance.

Guar gum, which provide highly viscous solutions at relatively low concentrations (less than 1% w/v), is widely used as emulsifier, thickener and stabilizer in various food products, such as ice cream, yogurt, and

***Corresponding author**
spnie@ncu.edu.cn

Received 24 June 2025
Received in revised from 26 August 2025
Accepted 6 November 2025

salad dressings [6]. In pharmaceutical formulations, guar gum is also used as a matrix former, release retardant, mucoadhesive agent, and colon-specific agent [7]. Guar gum is a linear, water-soluble galactomannan extracted from the guar bean, consisting of a (1–4)-linked β-D-mannose backbone with single (1–6)-bonded α-D-galactose side groups, with a mannose to galactose ratio of 2:1 [8]. Recent studies have shown that guar gum has great potential in improvements in lipid metabolism [9], autoimmune encephalomyelitis [10], and colitis [11]. Although the modulatory effects of guar gum on gut microbiota have been investigated, studies on its specific enrichment effects on particular bacterial strains and the interactions between the enriched bacteria and guar gum itself remain limited. In contrast, the fermentation characteristics of partially hydrolyzed guar gum have been more extensively reported [12, 13]. Given the widespread application of native guar gum in the food industry, a comprehensive investigation into its *in vitro* fermentation characteristics, as well as its selective enrichment of specific bacterial, is warranted.

In vitro simulation of gastrointestinal fermentation is a convenient and highly reproducible alternative approach, as it allows for the direct examination of the impact of dietary fibers on the microbial community structure without the complicating effects of host factors [14]. Although simulating colonic fermentation using fecal samples is a widely-used approach, the microbial composition of feces may differ from the actual conditions in the intestinal lumen due to the heterogeneous distribution of microbiota throughout the gastrointestinal tract [15]. In contrast, the use of colonic content samples can better represent the composition of the gut microbiome, thereby more accurately simulating the fermentation of dietary fibers within the intestinal environment.

Based on this, our study employed an *in vitro* colonic fermentation system to explore the modulatory effects of guar gum on gut microbiota. A significant enrichment of *Bifidobacterium* and *Parabacteroides* was observed, with particular enrichment of *B. pseudolongum* and *P. distasonis*. Given that both species were extensively reported to play crucial roles in gut homeostasis and host health [16, 17], highlighting the potential prebiotic effects of guar gum. Furthermore, single-step and stepwise culture systems were established to explore the interactions between guar gum and these two specifically enriched bacteria. The resulting data will contribute to a better understanding of the relationship between guar gum and gut microbiota and provide valuable insights for its application in food and pharmaceutical industries.

2. Materials and methods

2.1 Materials

Guar gum (Cat# C1013) were purchased from Sigma-Aldrich (St. Louis, MO, USA), and have been identified as a galactomannan (Figure 1A). Bacto-tryptone and yeast extract and were purchased from BD Difco (Franklin Lakes, NJ, USA). Acetate, propionate, and butyrate were of chromatographic grade. All other reagents used in this study were analytical grade and purchased from Sigma-Aldrich (St. Louis, MO, USA) or Aladdin (Shanghai, China).

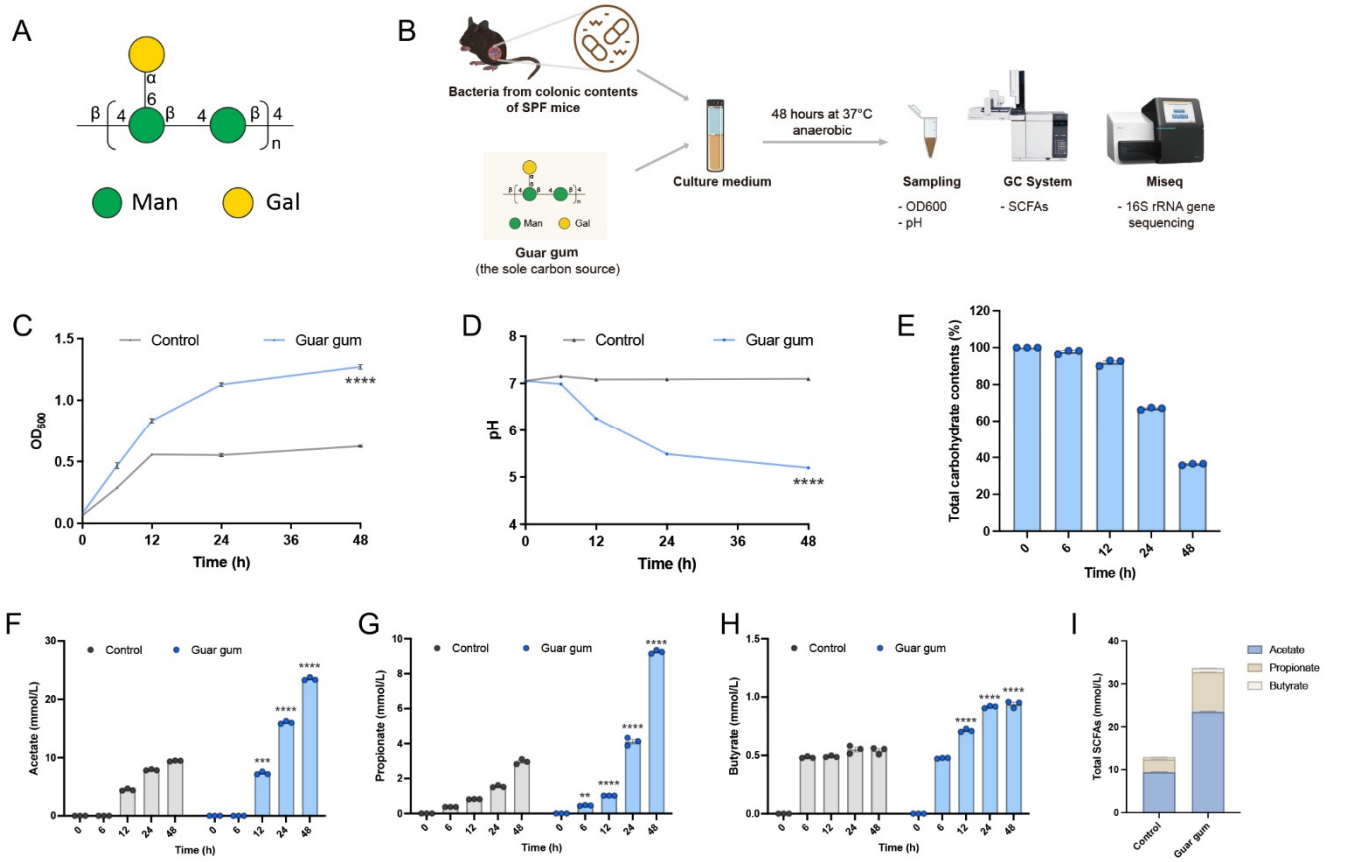

Figure 1. Guar gum is fermentable by the gut microbiota in the *in vitro* fermentation

(A) The structure of the repeating units of guar gum. (B) The schematic diagram for *in vitro* fermentation. (C-E) Changes in OD_{600}, pH, and total carbohydrates content during *in vitro* fermentation. (F-I) Changes in acetate, propionate, butyrate, and total SCFAs during *in vitro* fermentation. Data are presented as the mean ± SEM. n= 3 per group. ** $P < 0.01$, *** $P < 0.001$, **** $P < 0.0001$. For F-H, asterisks indicate a significant difference in SCFAs concentration between the guar gum group and the control group at the same sampling time point.

2.2 In vitro colonic fermentation

The basal medium was prepared according to a previously described method, with minor modifications [18]. Briefly, the basal medium consisted of 0.70 g/L acid-hydrolyzed casein, 1.17 g/L tryptone, 1.17 g/L Bacto-tryptone, 1.05 g/L yeast extract, 0.8 g/L L-cysteine hydrochloride, 0.4 g/L bile salts, 0.5 g/L KH_2PO_4, 1.5 g/L $NaHCO_3$, 4.5 g/L NaCl, 4.5 g/L KCl, 0.61 g/L $MgSO_4$, 0.1 g/L $CaCl_2 \cdot 2H_2O$, 0.005 g/L $FeSO_4 \cdot 7H_2O$, 0.01 g/L hemin, 1 mL Tween 80, 1 mL vitamin mixture, 1 mL vitamin mixture 2, 10 µL vitamin K_1, and 0.5 mL 0.2% resazurin, and 5g/L guar gum. The control group was maintained on the basal medium without guar gum. After adjusting the pH to 6.5, the medium was autoclaved at 121℃ for 15 min. The autoclaved culture medium, along with the necessary materials, was placed in the anaerobic chamber (5% H_2, 5% CO_2, and 90% N_2) and equilibrated for at least 12 h before inoculation to ensure an oxygen-depleted environment.

For fecal slurry preparation, colonic contents from healthy C57BL/6J male mice (6-weeks-old) were collected [19]. The mice were euthanized and the colonic contents were then immediately removed and transferred to an anaerobic chamber. Fecal slurries were prepared by homogenization with sterile pre-reduced phosphate buffer solution (PBS) containing 0.1% L-cysteine hydrochloride. The resulting mixture was thoroughly vortexed and then filtered through a sterile 100 µm cell strainer. This suspension

was inoculated at a 2% (v/v) ratio into the sterile culture medium, then incubated anaerobically at 37℃ with shaking for 48 h (Figure 1B). All animal use procedures were conducted in accordance with the National Research Council's Guide for the Care and Use of Laboratory Animals and were approved by the Experimental Animal Care and Use Committee of Nanchang University (Approval No. NCULAE-20221030020).

2.3 Sampling procedure

Samples were collected at 0, 24, and 48 h during the fermentation process. To maintain anaerobic conditions, all procedures were performed in an anaerobic chamber. The optical density (OD_{600}) of each sample was measured using a microplate reader at a wavelength of 600 nm. The pH of the samples was measured using a FiveEasy Plus FE28 pH meter (Mettler Toledo, Greisensee, Switzerland). The collected samples were stored at -80℃ until analysis. Three independent replicates were included at each time point.

2.4 Total carbohydrate contents determination

The total carbohydrate contents in the fermentation broth were determined using the phenol-sulfuric acid method [20]. The fermentation broth was centrifuged (8000 × g, 10 min), and 15 μL of the supernatant was collected. Subsequently, 500 μL of deionized water and 500 μL of 3% (w/v) phenol solution were added, followed by the slow addition of 2 mL of concentrated sulfuric acid, then vortexed to mix. After standing at room temperature for 30 minutes, a 200 μL portion was transferred to a microplate and the absorbance was measured at 490 nm. The total carbohydrate contents at 0 h of fermentation were set as 100%, and the remaining percentage of total carbohydrate contents at other time points was calculated and plotted to generate the change curve of total carbohydrate contents during the fermentation process.

2.5 Short-chain fatty acids (SCFAs) analysis

SCFAs were extracted from the fermentation broth using an esterification method as previously described [21]. Qualitative and quantitative analyses were performed according to the method described previously with minor modifications [22]. Briefly, fermentation samples were centrifuged at 12,000 × g for 10 min at 4℃ , and 0.5 mL of the supernatant was transferred to a screw-capped reaction vial. Subsequently, 1.2 mL of anhydrous ethanol, 0.1 mL of concentrated sulfuric acid, and 1 mL of n-hexane were added sequentially, followed by vortexing for 15 s. All steps were performed on ice. The sealed reaction vials were then placed in a shaking incubator at 60℃ and 200 r/min for 1 h to facilitate complete esterification. After cooling to room temperature, the upper organic layer was filtered through a 0.22 μm organic membrane filter. The SCFA composition and concentrations were determined using a gas chromatograph (Agilent 7890 B, Agilent Technologies, USA) equipped with an Agilent HP-5 column (30 m × 0.32 mm × 0.25 μm, Agilent 19091J-413). The chromatographic conditions were as follows: nitrogen was used as the carrier gas with a split ratio of 1:40; a flame ionization detector (FID) was employed; the temperature program started at 30℃ and held for 3.5 min, then increased to 40℃ at 5℃ /min, and further increased to 180℃ at

15℃ /min, holding at 180℃ for 10 min. The injection volume was 1 μL, and the injector temperature was 200℃ . The SCFAs concentrations in the samples were quantified by comparing their peak areas to calibration curves constructed using standard solutions of individual SCFAs.

2.6 DNA extraction and 16S rRNA gene sequencing

Total DNA was extracted from the fermentation broth using a Tiangen Stool DNA Extraction Kit. The concentration and purity of the extracted DNA were measured using a micro-volume spectrophotometer. The V4 region of the 16S rRNA gene was amplified by PCR (Bio-Rad, Hercules, CA, USA) using the 515 forward primer (5'-GTGCCAGCMGCCGCGGTAA-3') and 806 reverse primer (5'-GGACTACHVGGGTTCTAAT-3'). The integrity of the extracted DNA was verified by 1% (w/v) agarose gel electrophoresis. The PCR amplicons were purified using a Tiangen Agarose Gel DNA Purification Kit and quantified using a Qubit fluorometer (Thermo Fisher Scientific, Waltham, MA, USA). The amplicon libraries were sequenced on the Illumina MiSeq platform (Illumina, San Diego, CA, USA). The raw sequencing data were processed using QIIME2 (version 2020.11), where amplicon sequence variants (ASVs) were generated and taxonomically classified against the Greengenes reference database (version 13.8) using DADA2. Alpha and beta diversity analyses, as well as taxonomic profiling were conducted using MicrobiomeAnalyst (version 2.0). Linear discriminant analysis (LDA) effect size (LEfSe) analysis was performed by Galaxy to identify the major bacteria taxa enriched in different groups, and the effect size of the differentially abundant taxa was obtained through LDA based on the Kruskal-Wallis test with an α level of 0.05. Advanced correlation analysis and heatmap-bubble plot was performed using the OmicStudio tools available at https://www.omicstudio.cn/tool.

2.7 Bacterial strains and growth assays

Bifidobacterium pseudolongum ATCC 25526 and *Parabacteroides distasonis* ATCC 8503 were purchased from the American Type Culture Collection (ATCC). Following resuscitation and propagation, each bacterial strain was individually inoculated into YCFA medium containing guar gum, galactose, or mannose (0.2% w/v) as the sole carbon source or into YCFA medium without a carbon source. The composition of YCFA medium was as follows: 10 g/L casein peptone, 2.5 g/L yeast extract, 0.001 g/L resazurin, 0.45 g/L K_2HPO_4, 0.45 g/L KH_2PO_4, 0.9 g/L NaCl, 4.0 g/L $NaHCO_3$, 0.044 g/L $MgSO_4$, 0.09 g/L $CaCl_2$. The cultures were incubated anaerobically at 37℃ for 24 h. Samples were collected at the indicated time points and tested for OD_{600}, and $\triangle OD_{600}$ represents the difference in OD_{600} before and after incubation.

For stepwise culture assays, following resuscitation and propagation, *Bacteroides ovatus* ATCC 8483 was inoculated into YCFA medium supplemented with or without guar gum (0.2% w/v). After 12 h of anaerobic incubation at 37℃ , the cultures were centrifuged at 12,000 r/min for 5 min at 4℃ . The supernatant was collected, the pH was adjusted to 6.8, and the solution was sterilized by filtration through a 0.22 μm pore-size filter. Then, either *B. pseudolongum* or *P. distasonis* was inoculated into the treated supernatant and

cultured for 24 h. Samples were collected at the indicated time points and tested for OD_{600}, and $\triangle OD_{600}$ represents the difference in OD_{600} before and after incubation.

2.8 Statistical analysis

Statistical analysis and data visualization were conducted using GraphPad Prism (version 10.1.0). Student's *t*-test and One-way analysis of variance (ANOVA) with Tukey's post-hoc test was performed for differential analysis, with statistical significance set at $P < 0.05$. Data were presented as the mean ± standard error of the mean (SEM).

3. Results

3.1 Guar gum is fermentable by the gut microbiota

During the *in vitro* fermentation process, the OD_{600} value continued to rise and reached 1.2 after 48 h of fermentation, indicating that guar gum significantly promoted bacterial growth and proliferation. In contrast, in the control group without any added carbon source, the OD_{600} remained relatively stable at around 0.6 after 12 h of fermentation, revealing that bacterial proliferation was limited in the absence of a carbon source (Figure 1C).

Metabolites such as SCFAs produced by bacteria during fermentation have a strong influence on the pH of the intestinal environment. The results showed that with the degradation of guar gum, the pH of the fermentation broth gradually decreased from the initial 7.06 to 5.20 after 48 h of fermentation. This reflected the sustained metabolic activity of the bacteria (Figure 1D). Meanwhile, the pH of the fermentation broth in the control group remained relatively stable during the fermentation process, further indicating the potential role of guar gum in modulating the intestinal pH.

To further understand the degradation process of guar gum, we evaluated the degradation efficiency by monitoring the changes in the carbohydrate contents of the fermentation broth. The results showed that as the fermentation progressed, the content of guar gum in the fermentation broth gradually decreased, reaching a degradation rate of 63.69% after 48 h of fermentation (Figure 1E). This result not only confirms the degradability of guar gum but also provides important information for understanding its potential role in intestinal health.

3.2 Gut microbiota utilize guar gum to produce SCFAs

SCFAs, including acetate, propionate, and butyrate, are the main metabolites produced by gut microbiota during growth and proliferation on carbohydrates and provide health benefits to the host. The fermentation of guar gum significantly promoted acetate production (Figure 1F). Although no significant acetate production was detected during the initial fermentation period (0-6 h), the acetate levels steadily increased after 12 h of fermentation, reaching 23.49 mmol/L at 48 h, which was significantly higher than the 9.44 mmol/L observed in the control group. For propionate, the amount produced after 6 h of guar gum fermentation was already significantly higher than that in the control group, and this difference gradually increased as fermentation

progressed. After 48 h of fermentation, the propionate production in the guar gum group reached 9.25 mmol/L, which was 3.12 times higher than that in the control group (2.97 mmol/L) (Figure 1G). Guar gum fermentation also stimulated a significant increase in butyrate levels, with the guar gum group producing 0.94 mmol/L and and control group 0.54 mmol/L of butyrate after 48 h of fermentation (Figure 1H).

By summarizing the production of acetate, propionate, and butyrate, we found that guar gum fermentation significantly increased the total SCFAs production, which was mainly driven by the production of acetate and propionate (Figure 1I). This suggests that guar gum may primarily enrich gut bacteria that produce acetate and propionate.

3.3 Effect of guar gum on gut microbial composition

To investigate the influence of guar gum on bacterial composition, we employed 16S rRNA gene sequencing to examine the bacterial composition in the fermentation broth. α-diversity, which reflects the richness and evenness within a community, showed a decreasing trend during the fermentation process (Figure 2A, B). This suggests that fermentation may facilitate the enrichment of certain dominant bacterial taxa, thereby affecting the overall diversity. Notably, the Shannon index was significantly higher in the guar gum group compared to the control, indicating that the addition of guar gum promoted the enrichment of a greater number of species. β-diversity, which reflects differences in microbial community composition and distribution between samples, showed clear segregation of samples at different time points in the principal co-ordinate analysis (PCoA) plot (Figure 2C). Importantly, the difference between the guar gum group and control group gradually increased during the fermentation, indicating that the addition of guar gum had a sustained and significant effect on the bacterial community structure.

Through the analysis of the bacterial community composition at the phylum level, the guar gum treatment group was mainly composed of Firmicutes, Bacteroidetes, Proteobacteria, and Actinobacteria, while the control group was primarily composed of Firmicutes, Proteobacteria, and Bacteroidetes (Figure 2D). At the family level (Figure 2E), a significant enrichment of Enterobacteriaceae was observed in the control group, which was effectively suppressed by the guar gum treatment (Figure 2G). Additionally, the guar gum treatment significantly promoted the proliferation of bacteria such as Lactobacillaceae, Porphyromonadaceae, and Bifidobacteriaceae. At the genus level (Figure 2F), the abundance of *Bifidobacterium* was less than 0.02% at baseline (0 h) but increased significantly after fermentation of guar gum, reaching 7.86% and 8.36% at 24 h and 48 h, respectively (Figure 2H). Similarly, guar gum exhibited a strong enrichment effect on *Parabacteroides*, with its abundance continuously increasing during the fermentation process and reaching 32.36% at 48 h, nearly 10 times higher than the control group (3.40%) (Figure 2I). For the *Lactobacillus*, guar gum also demonstrated a certain enrichment effect, with higher enrichment observed at 24 h (24.44%) compared to 48 h (16.33%), implying that the primary proliferation phase of *Lactobacillus* occurred within the first 24 h of fermentation. During the subsequent 24 h, the relative abundance of *Lactobacillus* decreased, likely due to competition with other bacteria and the enrichment of other taxa (Figure 2J). Correlation analysis

of microbial communities and their association with SCFAs revealed strong correlations between *Parabacteroides* and *Bacteroides*, *Ruminococcus*, *Bifidobacterium*, and *Lactobacillus*. Additionally, acetate production showed significant positive correlations with *Bacteroides*, *Oscillospira*, and *Bifidobacterium*, while propionate levels were significantly positively correlated with *Bacteroides* and *Parabacteroides* (Figure 2K).

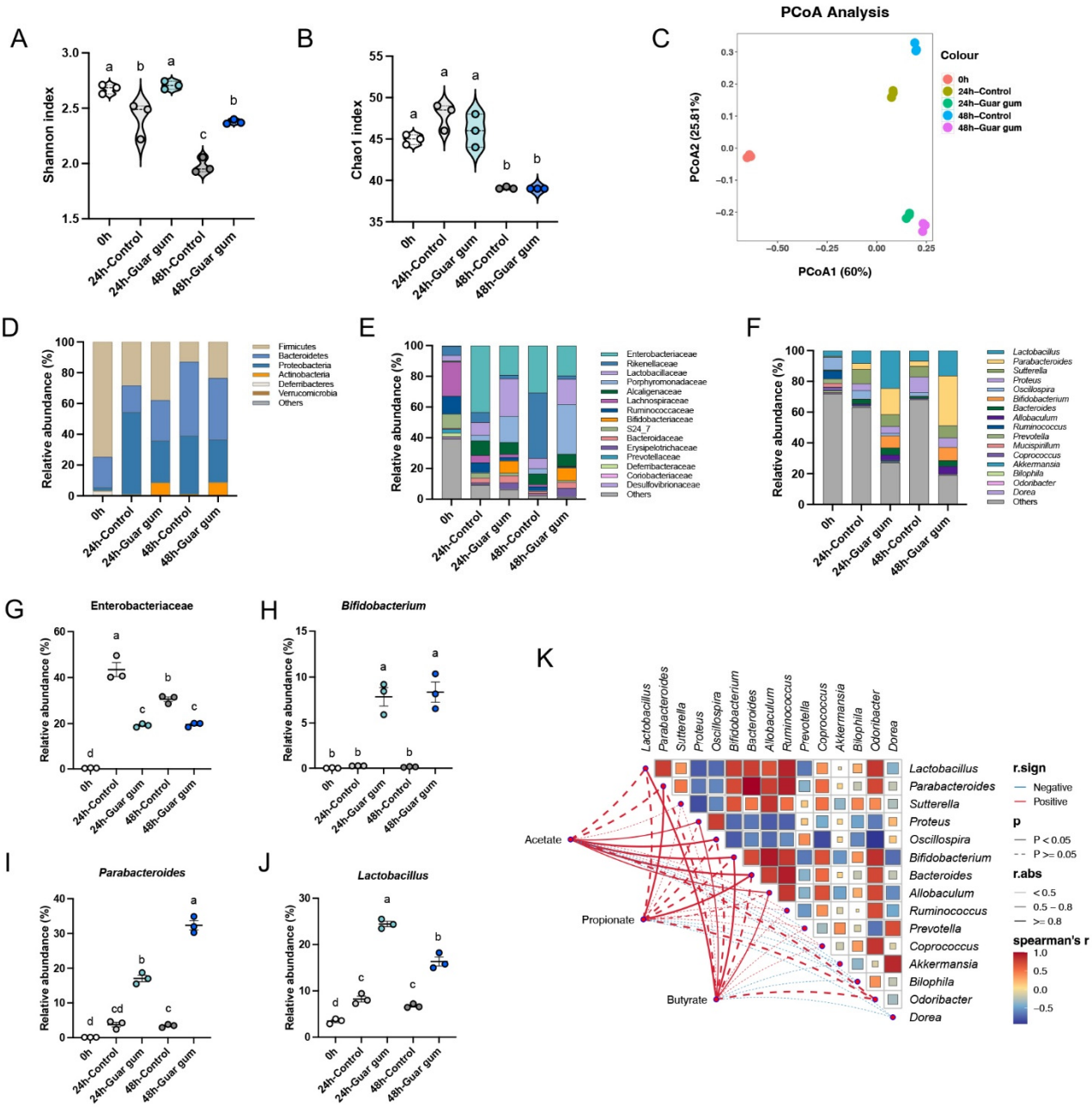

Figure 2. Effect of guar gum on gut microbial composition

(A, B) Alpha diversity, evaluated by Shannon and Chao1 index. (C) Principal co-ordinate analysis (PCoA) of microbiomes. (D-F) Taxonomic bacterial composition distribution at phylum, family, and genus levels. (G-J) Relative abundance of Enterobacteriaceae, *Bifidobacterium*, *Parabacteroides*, and *Lactobacillus*. (K) network heatmap analysis of correlation between microbial abundance and SCFAs levels (genus level, top 16; spearman's correlation coefficient > 0.8 or < −0.8, $P < 0.05$). Data are presented as the mean ± SEM. n= 3 per group. Statistical analysis was performed using one-way ANOVA followed by Tukey's post-hoc test, and different letters indicating significant differences between groups ($P < 0.05$).

3.4 The targeted enrichment effects of guar gum

To identify significant differences in microbial community composition between groups, LEfSe analysis was performed. The results showed that guar gum significantly enriched specific bacteria after 48 h of fermentation, including Porphyromonadaceae, *Parabacteroides distasonis*, Lactobacillaceae, *Bifidobacterium pseudolongum*, and *Lactobacillus*, while exhibiting a suppressive effect on bacteria such as *Rikenellaceae*, *Enterobacteriaceae*, and *Proteus*, which were enriched in the control group (Figure 3A, B).

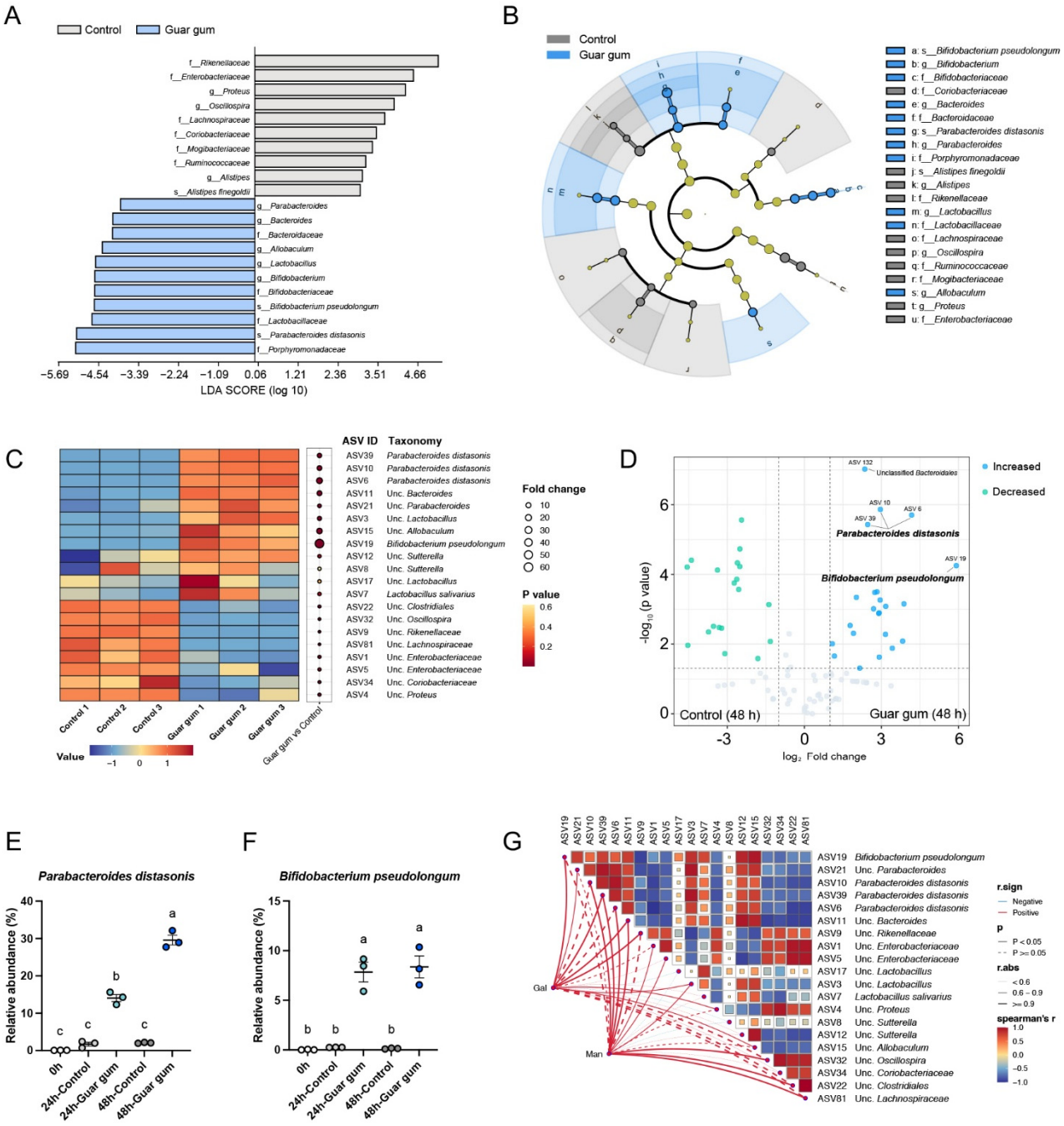

Figure 3. The targeted enrichment effects of guar gum

(A) Comparison of relative abundance of bacteria between Control (48 h) and Guar gum group (48 h) was calculated by linear discriminant analysis effect size (LEfSe). Taxa meeting an LDA score threshold > 2.0 is shown. (C) Heatmap-bubble plot analysis of the top 20 amplicon sequence variants (ASVs) based on their abundance. The heatmap (left panel) visualizes the

abundance levels of these ASVs across samples, with the color gradient reflecting relative abundance. The bubble plot (right panel) displays the fold change of each ASV's abundance in the guar gum group relative to the control group. (D) Volcano plot of ASVs between guar gum group and control group (48 h), with differential ASVs identified based on thresholds (dotted lines) of $|\log_2$ fold change$|> 1$ and $P < 0.05$. (E, F) Relative abundance of *P. distasonis* and *B. pseudolongum*. (G) network heatmap analysis of correlation between ASV abundance and monosaccharide contents (ASVs, top 20; spearman's correlation coefficient > 0.9 or < −0.9, $P < 0.05$). Data are presented as the mean ± SEM. n= 3 per group. Statistical analysis was performed using one-way ANOVA followed by Tukey's post-hoc test, and different letters indicating significant differences between groups ($P < 0.05$).

Using the top 20 abundant ASVs, guar gum primarily enriched *P. distasonis* (ASV6, ASV10, ASV39), *B. pseudolongum* (ASV19), and some unidentified *Bacteroides* and *Lactobacillus*. Among these, *B. pseudolongum* (ASV19) exhibited the most significant increase in abundance after fermentation, followed by *P. distasonis* (ASV6, ASV10, ASV39) (Figure 3C, D). As shown in the relative abundance results, after 48 h of fermentation, the abundance of *P. distasonis* reached 29.59% (a 14.33-fold increase compared to the control group), and the abundance of *B. pseudolongum* was 8.36% (a 60.20-fold increase compared to the control group) in the guar gum group (Figure 3E, F). These findings lead us to speculate that the structure of guar gum may be responsible for the targeted enrichment of these bacteria. Therefore, we conducted a correlation analysis between the monosaccharide content in guar gum measured earlier and bacterial abundance. Galactose was significantly positively correlated with *B. pseudolongum* (ASV19), *P. distasonis* (ASV39), and unclassified *Bacteroides* (ASV11), while mannose was significantly positively correlated with *P. distasonis* (ASV6, ASV10, ASV39) and unclassified *Bacteroides* (ASV11) (Figure 3G). Taken together, guar gum has a targeted enrichment effect on these potential beneficial bacterial species*, P. distasonis* and *B. pseudolongum*, which may be associated with its structural characteristics.

3.5 The enrichment of B. pseudolongum and P. distasonis requires a cross-feeding with primary degrader

To investigate whether *B. pseudolongum* and *P. distasonis* were selectively enriched through guar gum degradation capability, we conducted *in vitro* monoculture experiments (Figure 4A). The results revealed that neither *B. pseudolongum* nor *P. distasonis* could direct utilization of guar gum for growth (Figure 4B, C). This observation led us to hypothesize that primary degraders might mediate both guar gum breakdown and subsequent enrichment of *B. pseudolongum* or *P. distasonis*. Preliminary ASV analysis indicated a significant increase in unclassified *Bacteroides* following guar gum fermentation (Figure 3C), with strong positive correlations observed between the relative abundances of *Bacteroides* and those of *B. pseudolongum* and *P. distasonis* (Figure 4D, E). Given the rich array of glycoside hydrolases in *Bacteroides* [23], it is likely a key player in guar gum degradation. Studies have shown that *B. ovatus* efficiently utilizes guar gum for growth, whereas *Bacteroides uniformis* exhibits weaker utilization, and *Bacteroides thetaiotaomicron* and *Bacteroides caccae* show minimal growth on this substrate [24, 25]. These findings indicate that *B. ovatus* may be a key primary degrader of guar gum. Therefore, we performed quantitative PCR analysis and found that the abundance of *B. ovatus* in the culture medium significantly increased after guar gum fermentation (Figure 4F). Through *in vitro* culture, we confirmed that *B. ovatus* could efficiently utilize guar gum as a carbon source for growth and proliferation (Figure 4G).

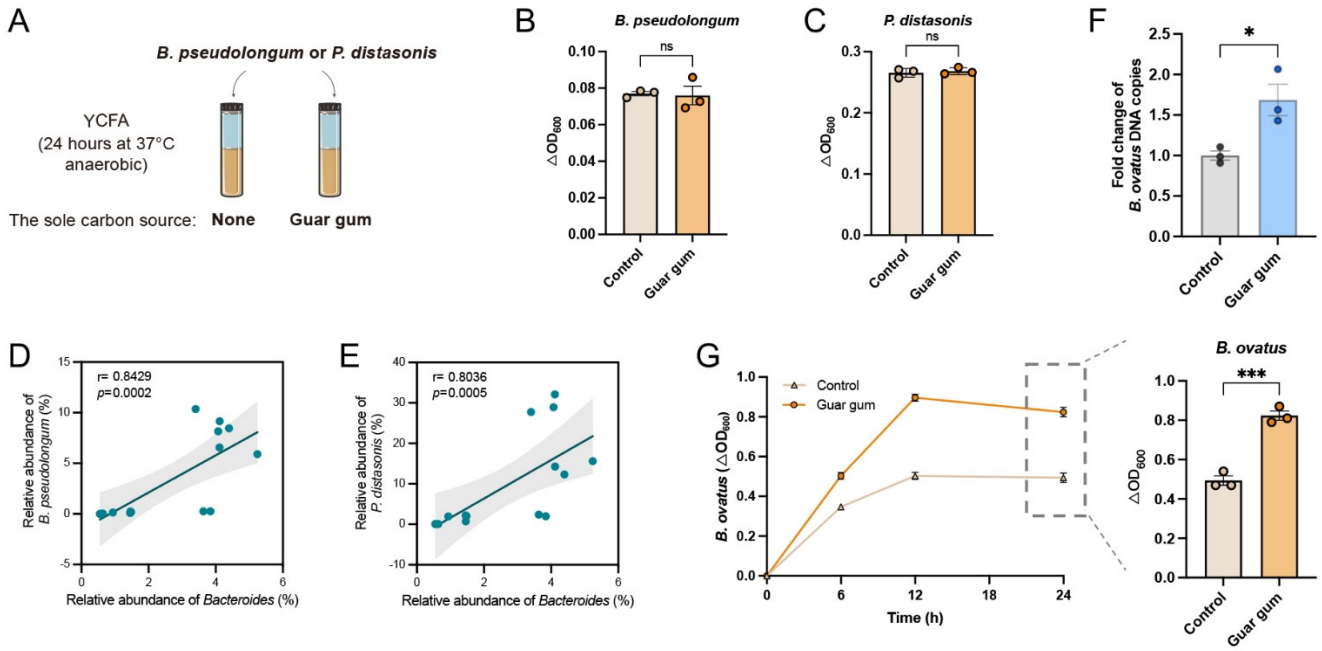

Figure 4. *B. pseudolongum* and *P. distasonis* cannot utilize guar gum

(A) Schematic diagram of the culture process, where the medium is YCFA medium with guar gum as the sole carbon source or carbon-free YCFA medium, inoculated with *B. pseudolongum* and *P. distasonis*, respectively. (B, C) The ΔOD_{600} values of *B. pseudolongum* and *P. distasonis*. (D, E) The spearman's correlation analysis between the relative abundance of *Bacteroides* and each of *B. pseudolongum* and *P. distasonis*. (F) Fold change in the abundance of *B. ovatus* in the guar gum group compared to the control group after *in vitro* fermentation. (G) Growth curves of *B. ovatus* in media with guar gum as the sole carbon source or without carbon source, and the OD_{600} values after 24 h of cultivation. Data are presented as the mean ± SEM. n= 3 per group. Statistical analysis was performed using *t*-test and one-way ANOVA followed by Tukey's post-hoc test. * $P < 0.05$, *** $P < 0.001$; no significant (ns) for $P > 0.05$.

Next, we ask whether guar gum degraded by *B. ovatus* could promote the proliferation of *B. pseudolongum* and *P. distasonis*. Subsequently, we conducted a stepwise co-culture system where filter-sterilized supernatants from *B. ovatus* cultures were inoculated with either *B. pseudolongum* or *P. distasonis* (Figure 5A). Both strains showed significant proliferation in the pre-cultured medium (1.72-fold and 1.5-fold increases respectively, $P < 0.05$), with *B. pseudolongum* demonstrating superior growth kinetics compared to *P. distasonis* (Figure 5B, C). Given that the main component of guar gum is a galactomannan and that *B. ovatus* possesses glycoside hydrolase (GH) 26 and GH36, which can release a large amount of galactose and mannose through the degradation of guar gum [24, 26]. Then we ask whether *B. pseudolongum* and *P. distasonis* could utilize galactose and mannose for growth. Through another monoculture experiment (Figure 5D), distinct substrate preferences were revealed: *B. pseudolongum* exhibited enhanced proliferation in galactose-supplemented media (3.98-fold compared to the control group), while *P. distasonis* showed preferential growth in mannose-enriched conditions (3.51-fold compared to the control group) (Figure 5E, F). Taken together, these findings highlight the critical role of primary degraders in mediating polysaccharide metabolism and target enrichment.

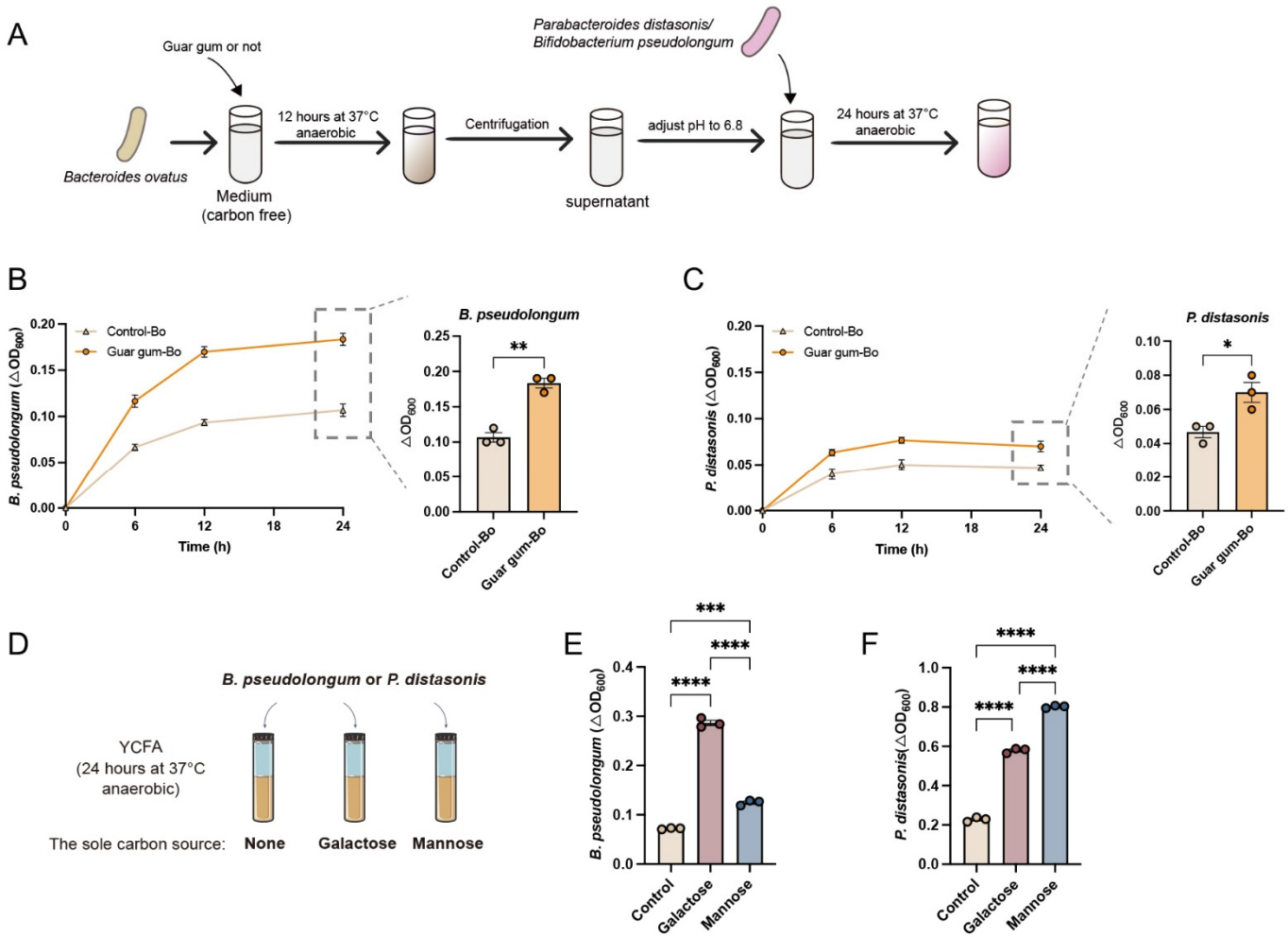

Figure 5. The enrichment of *B. pseudolongum* and *P. distasonis* requires a cross-feeding with primary degrader (A) Schematic diagram of stepwise co-culture. (B) Growth curves of *B. pseudolongum* in YCFA media with or without *B. ovatus* pre-culture for 12 h, and the OD_{600} values after 24 h of cultivation. (C) Growth curves of *P. distasonis* in YCFA media with or without *B. ovatus* pre-culture for 12 h, and the OD_{600} values after 24 h of cultivation. (D) Schematic diagram of the culture process, where the medium is YCFA medium containing galactose, mannose, or no carbon source, inoculated with *B. pseudolongum* and *P. distasoni*, respectively. (E, F) The ΔOD_{600} values of *B. pseudolongum* and *P. distasonis* after 24 h of cultivation. Data are presented as the mean ± SEM. n= 3 per group. Statistical analysis was performed using *t*-test and one-way ANOVA followed by Tukey's post-hoc test. * $P < 0.05$, ** $P < 0.01$, **** $P < 0.0001$.

4. Discussion

In this study, we found that guar gum exhibits prebiotic potential by suppressing *Enterobacteriaceae* while promoting *Bifidobacterium* and *Parabacteroides*. More importantly, guar gum had a targeted enrichment effect on certain bacteria, such as *B. pseudolongum* and *P. distasonis*, which required a cross-feeding with primary degrader. In addition, the degradation of guar gum induced gut microbiota to generate abundant acetate and propionate, which were related to the enrichment of *Bifidobacterium* and *Parabacteroides*.

The degradation of complex carbohydrates by gut microbiota results in the production of SCFAs, which can acidify the intestinal environment and play a pivotal role in regulating colonic physiology and altering the gut environment [27]. Consistent with our findings, the fermentation of guar gum and hydrolyzed guar gum using pig feces has been shown to promote the production of acetate, propionate, and butyrate [28]. In our

study, a significant increase in propionate production was observed within the first 6 h of fermentation, without a corresponding increase in acetate. This suggests that the proliferation of propionate-producing species may have been initially enhanced during the degradation of guar gum. Alternatively, acetate could have been immediately consumed through interspecies cross-feeding among bacteria, resulting in no significant change observed in its levels. Furthermore, butyrate was found to be significantly enriched during fermentation, which may be associated with the enrichment of certain butyrate-producing bacteria, such as *Faecalibacterium prausnitzii* [29] and *Roseburia intestinalis* [30]. These bacteria may potentially utilize fermentation by-products (acetate and succinate) produced by other bacteria for growth [31]. Correlation analysis revealed a strong positive association between butyrate and *Bifidobacterium*. As *Bifidobacterium* spp. are known acetate producers [32, 33], their activity may indirectly enhance butyrate synthesis by supporting the proliferation of butyrate-producing bacterial. Notably, *Bacteroides* and *Parabacteroides* demonstrated strong positive correlations with acetate and propionate. Given their established roles as primary producers of these SCFAs [34, 35], these findings confirmed that the production of acetate and propionate was linked to the metabolic activities of *Bifidobacterium*, *Bacteroides*, and *Parabacteroides*.

By analyzing the effects of guar gum on the gut microbiota, we found that it primarily suppresses the abundance of Enterobacteriaceae while promoting the abundance of *Bifidobacterium* and *Parabacteroides*. In one of our previous studies using gut microbiota from mice with colitis to ferment four food hydrocolloids, guar gum exhibited similar effects on the gut microbiota [20]. Enterobacteriaceae are a large family of Gram-negative bacteria that includes a number of pathogens, which are significantly enriched in patients with IBD [36]. The ability of guar gum to suppress the enrichment of these bacteria indicated its beneficial to intestinal health. Furthermore, the enrichment effect of guar gum on *Bifidobacterium* has also been similarly observed in *in vitro* fermentation using pig feces [28] and in *in vivo* intervention study in mice [37]. Partially hydrolyzed guar gum similarly induced the enrichment of *Bifidobacterium* and *Parabacteroides* during *in vitro* fermentation with feces from healthy humans [12, 38]. In a clinical intervention study, the daily intake of 8 g of guar gum for 18 consecutive days was found to increase the abundance of *Parabacteroides* as well as *P. distasonis* in the feces of healthy male subjects [6]. Further differential bacterial analysis revealed that *B. pseudolongum* and *P. distasonis* are the primary bacterial species enriched by guar gum. *B. pseudolongum*, a common probiotic, has been reported to ameliorate intestinal inflammation [39], liver disease-associated hepatocellular carcinoma [40], and enhance pulmonary immunity [41]. *P. distasonis* also exhibits a wide range of probiotic effects, including improving insulin resistance [42] and non-alcoholic steatohepatitis [43], holding the potential to be a next-generation probiotic.

Notably, our growth assays revealed that neither *B. pseudolongum* nor *P. distasonis* could directly utilize guar gum for growth. This aligned with previous findings showing that most *Bifidobacterium* species, including *B. pseudolongum*, lack the capacity to degrade guar gum [44]. Likewise, *P. distasonis* displayed minimal growth on mannans such as glucomannan [24]. This may be related to specific GHs in bacteria. In

contrast, *B. ovatus* encodes GH26 β-mannanases and GH36 α-galactosidase, which are mechanistically specialized for galactomannan degradation through synergistic endo- and exo-acting activities, ultimately releasing galactose and mannose [26, 45]. Our co-culture experiments demonstrated that *B. ovatus*-mediated guar gum degradation products robustly stimulated the growth of *B. pseudolongum* and *P. distasonis*. The impact of guar gum on gut microbiota may involve a "gear effect", where the presence of primary degraders facilitates the proliferation of other bacterial species [46]. Moreover, we revealed that *B. pseudolongum* had a preference for utilizing galactose, while *P. distasonis* had a preference for utilizing mannose. Studies have shown that bifidobacteria possessgenes encoding β-galactosidase (GH2 and GH42 families), and these enzymes can break down lactose and galactose, which explains their preference for galactose and is one of the reasons why bifidobacteria are dominant in the infant gut [47]. For *P. distasonis*, mannose and raffinose are important sources of energy [48]. The significant enrichment of *P. distasonis* after the fermentation of *Dendrobium*-derived glucomannans also indicated the potential role of mannose in the enrichment of *P. distasonis* [42, 49]. Regarding the observation that the products after *B. ovatus* degraded guar gum had a stronger promoting effect on the growth of *B. pseudolongum* than on *P. distasonis*, it is possible that the mannose produced by *B. ovatus* was limited. There may also have been other primary degraders involved in the degradation of guar gum and the release of mannose, which ultimately led to the enrichment of *P. distasonis*.

5. Conclusions

This study explored the effects of guar gum on the gut microbiota, highlighting its potential to targeted the enrichment of beneficial bacteria such as *B. pseudolongum* and *P. distasonis*, which may contribute to maintaining host health. Furthermore, the proliferation of *B. pseudolongum* and *P. distasonis* relied on primary degraders like *B. ovatus*, as they could not directly utilize guar gum. These findings advance our understanding of guar gum-microbiota interactions and offer valuable insights for designing microbiota-targeted functional foods. While our work outlines a cross-feeding framework where guar gum degraded by *B. ovatus* leads to specific enrichment, further research is warranted to fully understand the degradation mechanism of guar gum. Additionally, its targeted enrichment effects on gut microbiota, as well as its health benefits, need to be further verified in clinical studies.

Declaration of competing interest

The authors declare no competing interests.

Acknowledgments

This work was supported by the National Natural Science Foundation of China for the Key Project of International Cooperative Research (32120103012), the National Natural Science Foundation of China (32402115), the Technological Project of Jiangxi Province (20232BCD44003), and the Postdoctoral Fellowship Program and China Postdoctoral Science Foundation (GZB20230285; 2024M761264).

Data availability

Data will be made available on request.

References

[1] A. Vich Vila, J. Zhang, M. Liu, et al., Untargeted faecal metabolomics for the discovery of biomarkers and treatment targets for inflammatory bowel diseases, Gut. 73 (2024) 1909-1920.

[2] A.N. Ananthakrishnan, C.N. Bernstein, D. Iliopoulos, et al., Environmental triggers in IBD: a review of progress and evidence, Nature Reviews Gastroenterology & hepatology. 15 (2018) 39-49.

[3] H. Tilg, N. Zmora, T.E. Adolph, et al., The intestinal microbiota fuelling metabolic inflammation, Nature Reviews Immunology. 20 (2020) 40-54.

[4] N. Zmora, J. Suez, E. Elinav, You are what you eat: diet, health and the gut microbiota, Nat. Rev. Gastroenterol. Hepatol. 16 (2019) 35-56.

[5] S. Naimi, E. Viennois, A.T. Gewirtz, et al., Direct impact of commonly used dietary emulsifiers on human gut microbiota, Microbiome. 9 (2021) 1-19.

[6] C. Barber, C. Sabater, F. Guarner, et al., Metabolic response of intestinal microbiota to guar gum consumption, Frontiers in Nutrition. 10 (2023) 1160694.

[7] P.R. Guru, R.K. Kar, A.K. Nayak, et al., A comprehensive review on pharmaceutical uses of plant-derived biopolysaccharides, International Journal of Biological Macromolecules. 233 (2023) 123454.

[8] V.D. Prajapati, G.K. Jani, N.G. Moradiya, et al., Galactomannan: A versatile biodegradable seed polysaccharide, International Journal of Biological Macromolecules. 60 (2013) 83-92.

[9] T. Ghaffarzadegan, N. Marungruang, F. Fåk, et al., Molecular Properties of Guar Gum and Pectin Modify Cecal Bile Acids, Microbiota, and Plasma Lipopolysaccharide-Binding Protein in Rats, PLoS One. 11 (2016) e0157427.

[10] N.M. Fettig, H.G. Robinson, J.R. Allanach, et al., Inhibition of Th1 activation and differentiation by dietary guar gum ameliorates experimental autoimmune encephalomyelitis, Cell Reports. 40 (2022) 111328.

[11] S. Zhang, Y. Sun, Q. Nie, et al., Effects of four food hydrocolloids on colitis and their regulatory effect on gut microbiota, Carbohydrate Polymers. 323 (2024) 121368.

[12] J. Carlson, T. Gould, J. Slavin, In vitro analysis of partially hydrolyzed guar gum fermentation on identified gut microbiota, Anaerobe. 42 (2016) 60-66.

[13] S.J. Reider, S. Moosmang, J. Tragust, et al., Prebiotic Effects of Partially Hydrolyzed Guar Gum on the Composition and Function of the Human Microbiota—Results from the PAGODA Trial, Nutrients. 12 (2020) 1257.

[14] H. Ji, J. Hu, S. Zuo, et al., In vitro gastrointestinal digestion and fermentation models and their applications in food carbohydrates, Critical Reviews in Food Science and Nutrition. 62 (2022) 5349-5371.

[15] G. McCallum, C. Tropini, The gut microbiota and its biogeography, Nature Reviews Microbiology. 22 (2024) 105-118.

[16] W.K.K. Wu, Parabacteroides distasonis: an emerging probiotic?, Gut. 72 (2023) 1635-1636.

[17] Y. Xiao, J. Zhao, H. Zhang, et al., Colonized niche, evolution and function signatures of Bifidobacterium pseudolongum within bifidobacterial genus, Foods. 10 (2021) 2284.

[18] S.A. Poeker, C. Lacroix, T. De Wouters, et al., Stepwise development of an in vitro continuous fermentation model for the murine caecal microbiota, Front. Microbiol. 10 (2019) 1166.

[19] S. Zhang, Q. Nie, Y. Sun, et al., Bacteroides uniformis degrades β-glucan to promote Lactobacillus johnsonii improving indole-3-lactic acid levels in alleviating colitis, Microbiome. 12 (2024) 177.

[20] S. Zhang, Y. Sun, Q. Nie, et al., In vitro assessment of the effect of four polysaccharides on intestinal bacteria of mice with colitis, Food Frontiers. 4 (2023) 1462-1471.

[21] Y. Sun, J. Hu, S. Zhang, et al., Prebiotic characteristics of arabinogalactans during in vitro fermentation through multi-omics analysis, Food and Chemical Toxicology. 156 (2021) 112522.

[22] Y.E. Tuncil, C.H. Nakatsu, A.E. Kazem, et al., Delayed utilization of some fast-fermenting soluble dietary fibers by human gut microbiota when presented in a mixture, Journal of Functional Foods. 32 (2017) 347-357.

[23] P. Lapébie, V. Lombard, E. Drula, et al., Bacteroidetes use thousands of enzyme combinations to break down glycans, Nature communications. 10 (2019) 2043.

[24] Z. Qu, H. Liu, J. Yang, et al., Selective utilization of medicinal polysaccharides by human gut Bacteroides and Parabacteroides species, Nature Communications. 16 (2025) 638.

[25] M.S. Desai, A.M. Seekatz, N.M. Koropatkin, et al., A dietary fiber-deprived gut microbiota degrades the colonic mucus barrier and enhances pathogen susceptibility, Cell. 167 (2016) 1339-1353. e1321.

[26] S.K. Reddy, V. Bågenholm, N.A. Pudlo, et al., A β-mannan utilization locus in Bacteroides ovatus involves a GH36 α-galactosidase active on galactomannans, FEBS letters. 590 (2016) 2106-2118.

[27] A.S. Weiss, L.S. Niedermeier, A. von Strempel, et al., Nutritional and host environments determine community ecology and keystone species in a synthetic gut bacterial community, Nature Communications. 14 (2023) 4780.

[28] X. Fu, X. Wei, M. Xiao, et al., Properties of hydrolyzed guar gum fermented in vitro with pig fecal inocula and its favorable impacts on microbiota, Carbohydrate Polymers. 237 (2020) 116116.

[29] Z. Shi, M. Li, C. Zhang, et al., Butyrate-producing Faecalibacterium prausnitzii suppresses natural killer/T-cell lymphoma by dampening the JAK-STAT pathway, Gut. 0 (2024) 1-14.

[30] X. Kang, C. Liu, Y. Ding, et al., Roseburia intestinalis generated butyrate boosts anti-PD-1 efficacy in colorectal cancer by activating cytotoxic CD8+ T cells, Gut. 72 (2023) 2112-2122.

[31] E.R. Mann, Y.K. Lam, H.H. Uhlig, Short-chain fatty acids: linking diet, the microbiome and immunity, Nature Reviews Immunology. 24 (2024) 577-595.

[32]C. Zhang, L. Yu, C. Ma, et al., A key genetic factor governing arabinan utilization in the gut microbiome alleviates constipation, Cell Host & Microbe. 31 (2023) 1989-2006. e1988.

[33] Q. Song, X. Zhang, W. Liu, et al., Bifidobacterium pseudolongum-generated acetate suppresses non-alcoholic fatty liver disease-associated hepatocellular carcinoma, Journal of Hepatology. 79 (2023) 1352-1365.

[34] X. Wang, Z. Cai, Q. Wang, et al., Bacteroides methylmalonyl-CoA mutase produces propionate that promotes intestinal goblet cell differentiation and homeostasis, Cell Host & Microbe. 32 (2024) 63-78. e67.

[35] H. Ma, L. Yang, Y. Liang, et al., B. thetaiotaomicron-derived acetic acid modulate immune microenvironment and tumor growth in hepatocellular carcinoma, Gut Microbes. 16 (2024) 2297846.

[36] J.-Y. Lee, S.A. Cevallos, M.X. Byndloss, et al., High-Fat Diet and Antibiotics Cooperatively Impair Mitochondrial Bioenergetics to Trigger Dysbiosis that Exacerbates Pre-inflammatory Bowel Disease, Cell Host & Microbe. 28 (2020) 273-284.e276.

[37] D. Paudel, D.V.T. Nair, S. Tian, et al., Dietary fiber guar gum-induced shift in gut microbiota metabolism and intestinal immune activity enhances susceptibility to colonic inflammation, Gut Microbes. 16 (2024) 2341457.

[38] X.-E. Pi, H. Fu, X.-X. Yang, et al., Bacterial, short-chain fatty acid and gas profiles of partially hydrolyzed guar gum in vitro fermentation by human fecal microbiota, Food Chemistry. 430 (2024) 137006.

[39] W. Guo, B. Mao, S. Cui, et al., Protective Effects of a Novel Probiotic Bifidobacterium pseudolongum on the Intestinal Barrier of Colitis Mice via Modulating the Pparγ/STAT3 Pathway and Intestinal Microbiota, Foods. 11 (2022) 1551.

[40] Q. Song, X. Zhang, W. Liu, et al., Bifidobacterium pseudolongum-generated acetate suppresses non-alcoholic fatty liver disease-associated hepatocellular carcinoma, Journal of Hepatology. 79 (2023) 1352-1365.

[41] Y.J. Kim, J.-Y. Lee, J.J. Lee, et al., Arginine-mediated gut microbiome remodeling promotes host pulmonary immune defense against nontuberculous mycobacterial infection, Gut Microbes. 14 (2022) 2073132.

[42] Y. Sun, Q. Nie, S. Zhang, et al., Parabacteroides distasonis ameliorates insulin resistance via activation of intestinal GPR109a, Nature Communications. 14 (2023) 7740.

[43] W. Wei, C.C. Wong, Z. Jia, et al., Parabacteroides distasonis uses dietary inulin to suppress NASH via its metabolite pentadecanoic acid, Nature Microbiology. 8 (2023) 1534-1548.

[44] F. Crociani, A. Alessandrini, M.M. Mucci, et al., Degradation of complex carbohydrates by Bifidobacterium spp, International Journal of Food Microbiology. 24 (1994) 199-210.

[45] X. Wang, X. Yan, Y. Liu, et al., Preparation and identification of galacto-mannooligosaccharides generated from guar gum by a recombinant β-mannanase from Bacteroides fragilis (BF0736), Food Hydrocolloids. 152 (2024) 109893.

[46] Y. Sun, S. Zhang, J. Yin, et al., Bioactive Polysaccharides Targeting Gut Microbiota to Modulate Host Health: A Gear Effect Theory, Food Frontiers. (2025)

[47]C. Milani, G.A. Lugli, S. Duranti, et al., Bifidobacteria exhibit social behavior through carbohydrate resource sharing in the gut, Scientific reports. 5 (2015) 15782.

[48] J.C. Ezeji, D.K. Sarikonda, A. Hopperton, et al., Parabacteroides distasonis: intriguing aerotolerant gut anaerobe with emerging antimicrobial resistance and pathogenic and probiotic roles in human health, Gut microbes. 13 (2021) 1922241.

[49]Y. Sun, S. Zhang, H. He, et al., Comprehensive evaluation of the prebiotic properties of Dendrobium officinale polysaccharides, β-glucan, and inulin during in vitro fermentation via multi-omics analysis, International Journal of Biological Macromolecules. 253 (2023) 127326.